Nonlinear current-voltage and dielectric properties of $CaCu_3Ti_4O_{12}$ ceramics prepared by an aloe vera solution method

Sasitorn Putjuso[1], Sunan Nonglek[2] and Thanin Putjuso[1*]

Abstract

Nonlinear current-voltage characteristic and dielectric properties of $CaCu_3Ti_4O_{12}$ (CCTO) ceramics prepared from $CaCu_3Ti_4O_{12}$ nanopowder obtained by the aloe vera solution method are investigated. The XRD results of CCTO nanopowder and CCTO ceramics indicated a perovskite structure with the observed impurity phases of $CaTiO_3$ and CuO in all samples. The maximum dielectric constant (ε') measured at 30 °C and 1 kHz was found to be 1.10×10^4 with the minimum loss tangent ($\tan\delta$) of 0.07 for a CCTO ceramic sintered at 1050 °C. Non-ohmic properties with a high breakdown field (E_b) of 2,215 $V.cm^{-1}$ and a large nonlinear coefficient (α) of 19.31 were observed in a CCTO ceramic sample sintered at 1020 °C. The dielectric, $\tan\delta$, and non-ohmic properties were found to be associated with the microstructure of the $CaCu_3Ti_4O_{12}$ ceramics.

Keywords: nonlinear current-voltage, dielectric properties, $CaCu_3Ti_4O_{12}$, aloe vera solution method

[1] School of General Science, Faculty of Liberal Arts, Rajamangala University of Technology Rattanakosin, Wang Klai Kangwon Campus, 77110, Thailand

[2] Faculty of Industrial and Technology, Rajamangala University of Technology Rattanakosin, Wang Klai Kangwon Campus, 77110, Thailand

* Corresponding author. E-mail: thanin.put@rmutr.ac.th

Introduction

Over a decade of years, perovskite $CaCu_3Ti_4O_{12}$ (CCTO) hads attracted much attention because of its intriguing properties of high dielectric constant and applicable potential for microelectronic devices. Synthesis of CCTO was firstly reported by Subramanian *et al*. (2000) with high dielectric permittivity of about 10^4–10^5 at the low frequency and the room temperature (Subramanian *et al*., 2000; Homes *et al*., 2001). In addition, it was stable over a wide range of temperature from -173 °C to 327 °C (Mu *et al*., 2009). However, below -173 °C, the dielectric constant dropeds rapidly to around 100 without any structural phase transition (Sinclair *et al*., 2002). So far, the explanations for the origin of the giant dielectric property of CCTO material had been proposed with the controversial based on the intrinsic properties of the material and the extrinsic effects. Although several previous works had reported that the giant dielectric response of this material was found to be very sensitive to its microstructure i.e. grain size and the processing conditions such as sintering temperature and time, cooling rate and partial pressure in some preparation techniques (Chung *et al*., 2004; Adams *et al*., 2006; Krohns *et al*., 2008; Lunkenheimer *et al*., 2010), there were some investigations, which tended to support the concept that a high dielectric constant was originated from the extrinsic effects i.e. the internal barrier layer capacitor (IBLC) (Sinclair *et al*., 2002; Chung *et al*., 2004; Adams *et al*., 2006; Krohns *et al*., 2008), contact-electrode effected (Liu *et al*., 2006; Ramirez *et al*., 2009) and the in homogeneity of the local dielectric responsibility (Jha *et al*., 2003). At the present, the IBLC explanation of an extrinsic mechanism is widely accepted (Jin *et al*., 2007; Thongbai *et al*., 2012; Almeida *et al*., 2014). Besides the giant dielectric property, this material can also exhibit nonlinear electrical behavior due to the existence of the intrinsic potential barriers at the grain boundaries (GBs) i.e. the Schottky effect, making it suitably for application in varistors (Chung *et al*., 2004; Ramirez *et al*., 2009). Recently, many researchers had paid more attention on the study of the dependence of the nonlinear current–voltage (current density–electric field, J–E) properties of the CCTO material on the preparation technique with many interesting results (Chung *et al*., 2004; Liu *et al*., 2011; Thongbai *et al*., 2012; Xue *et al*., 2015).

In previous studies, CCTO ceramics had been generally prepared by the standard solid-state reaction method (Subramanian *et al*., 2000; Homes *et al*., 2001). According to this method, a powder of each starting material

usually hads a size in a micro scale and it requireds many hours of grinding during the powder preparation process. Moreover, the obtained product usually suffereds from the disadvantage of in homogeneity. On the other hand, a synthesis of CCTO precursor powder from a solution afforded the reaction with a homogeneous mixing of the metal ions at the atomic level and a shorter reaction time (Lunkenheimer *et al*., 2010). Nowadays, several research groups were interested in the preparation of CCTO nanopowders from a solution method by using different starting materials, solution reagents and conditions (Jesurani *et al*., 2011). From these works, it was remarkable that in addition to a strictly controlled synthesis environment and the expensive reagents used, many toxic solvents are involved in the process. Consequently, the searching and development of the alternative synthesis process by using inexpensive, nontoxic and environmentally benign precursors were still the key issues. One way that many researchers had proposed for the clean environment and the reduction of some toxic reagents was the use of a natural product extracted from plant as a part of a solvent during the synthesis of the material. In general, one of the most interesting plant widely used for this purpose was aloe vera (Choi and Chung, 2003), because it possesseds a unique property of immunomodulatory, anti-inflammatory, UV protection, and antiprotozoal, especially for wound and burn healings (Reynolds and Dweck, 1999), and it could be functioned as a bio-reducing agent to associate the metal ions in solution (Amalraj *et al*., 2013).

Recently, the extract of an aloe vera plant hads been successfully used to synthesize the single crystalline triangular gold nanoparticles (~50-350 nm in size) and the spherical silver nanoparticles (~15 nm in size) in a high yield by the reaction of an aqueous metal sources of Au and Ag ions in the extract solution of an aloe vera plant (Chandran *et al*., 2006). Most recently, some researchers had reported the synthesis of several kinds of nanopowders with particle sizes in the range of 5-50 nm (Maensiri *et al*., 2008), including nanoparticles of hydroxyapatite (Klinkaewnarong *et al*., 2010) and ferrites (MFe_2O_4, M = Ni, Cu, Zn and (Ni-Cu-Zn) Fe_2O_4) (Laokul *et al*., 2011) by using the aloe vera solution route. This method was simple, cost effective and environmental benign, as well as a promising synthesis route for preparation of fine ceramic particles. It was suggested that an aloe vera extract function as a complexing agent in the modified solution route. Thus, it was of great interest to elucidate the electrical properties and

nonlinear current-voltage of CCTO ceramics prepared by sintering the CCTO nonopowder obtained by the aloe vera solution route.

In this paper, we the researchers reported the preparation of CCTO ceramics by sintering the 850 °C-precalcined CCTO nanopowder obtained by the simple aloe vera solution route at the appropriate temperatures of 1020 and 1050 °C for 6h in air. The effects of sintering temperature on the microstructure, dielectric response, electrical properties, and nonlinear characteristic of the CCTO ceramics were systematically investigated. The results revealed that the CCTO ceramics exhibit giant dielectric with low loss tangent ($\tan\delta$) and nonlinear properties were closely related to the CCTO microstructural.

Methodology

In this work, copper nitrate ($Cu(NO_3)_2.3H_2O$, 99.5% Carlo Erba), calcium nitrate ($Ca(NO_3)_2.4H_2O$, 99.99% Kanto), titanium solution ($C_{16}H_{28}O_6Ti$, 99.8% Sigma Aldrich) were used as the starting materials. The aloe vera extracted solution was prepared from a 350 g portion of thoroughly washed aloe vera leaves, which were finely cut and boiled at 80 °C in 1000 ml of deionized water using mechanical stirring until a homogeneous solution was obtained. The aloe vera solution was left to cool and the residual fibrous was filtered out. According to the stoichiometric formula of $CaCu_3Ti_4O_{12}$, each metal nitrate and titanium solution were slowly added into the aloe vera solution with vigorous stirring for a further 2 h to obtain a well-dissolved solution. Then, the mixed solution was evaporated by heating on a hot plate at 150 °C with vigorous stirring for several hours until a gel precursor was obtained. The gel precursor was precalcined to dry at 400 °C for 2 h in a box furnace. The dried gel was crushed and ground into fine powder using an agate mortar. It was then calcined at 850 °C for 4 h in air (denoted as P-850). The P-850 powder was pressed into several pellets of 9.5 mm in diameter and approximately 1-2 mm in thickness by a uniaxial compression method at 150 MPa. These pellets were sintered at two different temperatures of 1020 °C and 1050 °C for 6 h in air and they were referred to the CCTO-1 and CCTO-2 ceramic, respectively. The density of each ceramic was measured by Archimedes method. The structure and phase of CCTO nanopowder and ceramics were characterized by X-ray diffraction (PW3040 Philips X-ray diffractometer with CuK_α radiation (λ= 0.15406 nm), the Netherlands). The morphology of both ceramics was studied using scanning electron microscopy (LEO SEM VP1450, UK). The average grain size of each

CCTO ceramic was measured using a standard line intercept technique from SEM micrograph of each sample. The electrode of each ceramic pellet was prepared by subsequently polished, ultrasonic cleaned, dried and coated with silver paint on both sides of the surfaces. The dielectric and electrical properties of both ceramics were measured using a Hewlett Packard 4194A impedance gain phase analyzer over a wide range of frequency (100Hz-1MHz) and temperature (-50 to 200 °C) at an oscillation voltage of 1.0 V. During the measurement, temperature was kept constant with an accuracy of ±1 °C. The current-voltage measurements were performed in a temperature range from 24 °C to 80 °C, using a high voltage measurement unit (Keithley Model 247). Prior to measurements, Au electrodes were made on both surfaces of each pellet using a Polaron SC500 sputter coating unit. The breakdown field (E_b) was obtained at a current density (J) of 1 mA.cm^{-2}. The nonlinear coefficient (α) values were calculated by the following equation,

$$\alpha = \frac{\log(J_2 / J_1)}{\log(E_2 / E_1)} \qquad (1)$$

Where E_1 and E_2 are the electric fields corresponding to J_1 = 1 and J_2 = 10 mA.cm^{-2}, respectively.

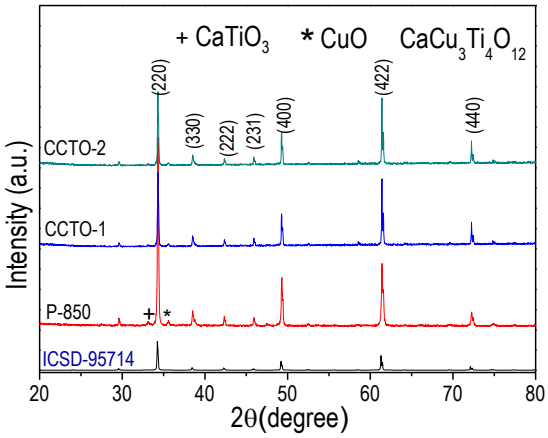

Figure 1 XRD patterns of the P-850, CCTO-1 and CCTO-2 samples compared to that of the standard data of CCTO (ICSD-95714).

Results and discussion

(Figure 1) showeds the XRD patterns of the CCTO powder (P-850), sintered CCTO ceramic samples (CCTO-1 and CCTO-2) and the standard CCTO (ICSD card No.95714). The XRD results confirmed the perovskite structure of all samples with the observed second phases of $CaTiO_3$ (ICSD card No.96679) and CuO (ICSD card No.26715). The presence of $CaTiO_3$ in the P-850 powder was suggested to come from an excess of titanium in the solution even if there was no excess of calcium (Guillemet-Fritsch *et al.*, 2006). Consequently, the CuO phase was then formed due to the deviation of the components from the stoichiometric formula. Possibly, the Cu rich phase might be derived from the diffusion of Cu to the defects present, after which gross excess causes the crystallization of

the separate CuO phase (Capsoni *et al*., 2004). However, both of the second phases were decreased with increasing sintering temperature, as revealed by the decrease of the XRD peak intensities of both phases shown in (Figure 1). This result indicateds that the sintering temperature can affect the formation of CCTO ceramics. The existences of CuO phase in CCTO-1 and CCTO-2 ceramics were similar to that reported by Capsoni *et al*. (2004). From the X-ray line broadening of the main peaks (220), (400), (422) and (440), the average crystallite size of the P-850 powder was calculated using the Scherrer's formula (Thongbai *et al.,* 2012) and it is found to be 60.1±5.0 nm. The calculated lattice parameters *a* of the P-850, CCTO-1 and CCTO-2 samples using the Rietveld program (Ni and Chen, 2007) were found to be 7.3907(3), 7.3897(3) and 7.3937(3) Å, respectively. These values were comparable to those reported in the literature (Thongbai *et al.,* 2012) and ICSD card no. 95714 for standard CCTO (7.391 Å). By using Rietveld method the X-ray density of the P-850 powder was found to be 5.0530 g.cm^{-3}. The relative densities of CCTO-1 and CCTO-2 ceramics measured by the Archimedes method are found to be 87.3% and 89.5%, respectively. Using the Rietveld method, the calculated density of CCTO ceramic is 5.056 g.cm^{-3}. The relative density, X-ray density and lattice parameter of these samples were listed in (Table 1).

Table 1 Relative density (R_d), X-ray density using Rietveld method and lattice parameter of CCTO samples.

samples	R_d(g.cm^{-3})	lattice parameter (Å)	X-ray density (g.cm^{-3})
P-850	-	7.3907(3)	5.053
CCTO-1	87.3	7.3897(3)	5.047
CCTO-2	89.5	7.3937(3)	5.055

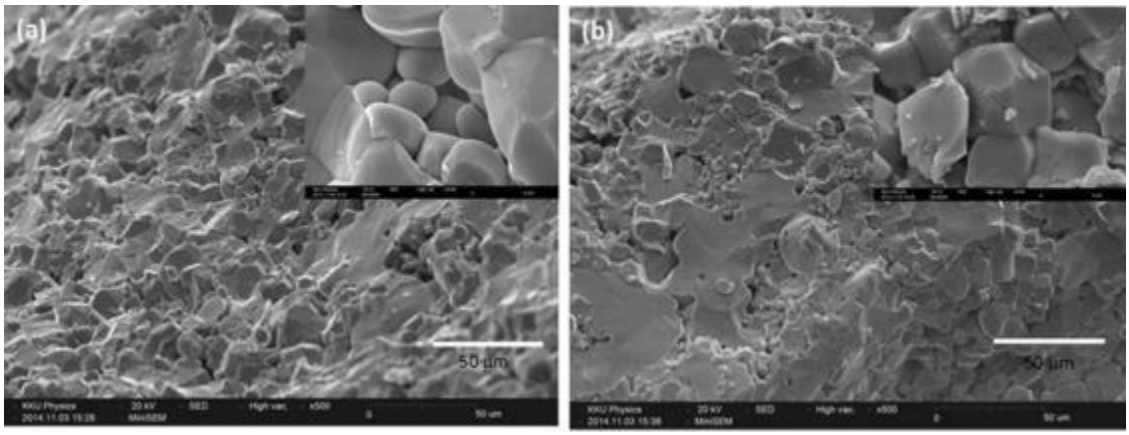

Figure 2 SEM micrographs of the fractured surface of (a) CCTO-1 and (b) CCTO-2 ceramics; the insets show the expanded view of each ceramic.

(Figure 2a and 2b) showed the fractured surface morphologies of the CCTO-1 and CCTO-2 ceramics, respectively. It could be seen in (Figure 2a and 2b), the microstructures of both CCTO-1 and CCTO-2 ceramics were similar and dense with larger grain observed in CCTO-2. The grain growth mechanism of these two ceramics was related to mass transport across GBs by diffusion of ions across the GB region, resulting in the movement of the GBs. During the sintering process, the existence of liquid phase in microstructure of both ceramics could enhance the diffusion rate of ions, leading to a great enhancement of the GB mobility and densification similar to that reported in the literatures (Chung *et al*., 2004; Adams *et al*., 2006; Krohns *et al*., 2008). The average grained size of CCTO-1is estimated from a SEM micrograph in (Figure 2a) and it was found to be 7.5 ± 2.6 μm, whereas that of the CCTO-2 in (Figure 2b) is about 11.0 ± 3.4 μm with a dense microstructure.

The frequency dependence of the dielectric constant (ε') and loss tangent (tan δ) of CCTO-1 and CCTO-2 ceramics at 30 $^{\circ}$C and 1 kHz are shown in (Figure 3a). In (Figure 3a), the observed ε' and tan δ values of the CCTO-1 are 9.87×10^{3} and 0.087, respectively. In the case of CCTO-2, these values were 1.10×10^{4} and 0.077, respectively. In the present study, it was obvious that the CCTO-2 had a higher dielectric constant than that of the CCTO-1 due to the belonging of denser microstructure and larger grain of the CCTO-2, corresponding to the higher relative density of CCTO-2. Additionally, the tan δ value of the CCTO-2 was lower than that of the CCTO-1, according to the higher grain boundary resistance (R_{gb}) of the CCTO-2 than that of the CCTO-1, as shown in the inset (a1) of (Figure 4). In (Figure 3a),

the lowest tanδ value of 0.08 for CCTO-1 and 0.04 for CCTO-2 were occurred at the frequencies of 1.4×10^3 and 4.6×10^3 Hz, respectively. These results suggested that CCTO ceramics prepared by sintering the CCTO nanopowder obtained by the aloe vera solution method might have a potential for the capacitor application. The values of ε' and tanδ at 30 °C and 1 kHz for both CCTO-1 and CCTO-2 ceramics were listed in (Table 2).

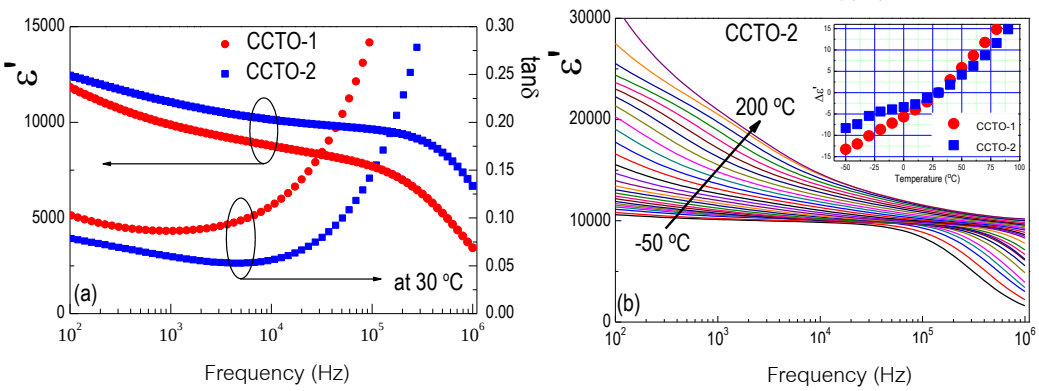

Figure 3 (a) Frequency dependence of ε' and loss tangent (tanδ) at 30 °C and 1 kHz of CCTO-1 and CCTO-2 ceramics and (b) frequency dependence of ε' of CCTO-2 ceramic in a temperature range of -50 to 200 °C; inset shows the temperature coefficient ($\Delta\varepsilon'$) evaluated at the frequency of 1 kHz of both CCTO-1 and CCTO-2 ceramics in a temperature range of -50 to 100 °C.

Table 2 Grain boundary resistance (R_{gb}) at 100 °C, dielectric constant (ε') and loss tangent (tanδ) at 30 °C and 1 kHz, nonlinear coefficient (α), and breakdown field (E_b) of the CCTO-1 and CCTO-2 ceramics.

samples	R_{gb}(Ω.cm)	ε'	tanδ	α	E_b(V.cm^{-2})
CCTO-1	2×10^6	9,870	0.087	19.31	2,215
CCTO-2	3×10^6	11,000	0.077	6.37	1,010

It is widely accepted that, the giant dielectric properties of both CCTO ceramics couldan be ascribed base on the internal barrier layer capacitor (IBLC) model (Sinclair *et al*., 2002; Chung *et al*., 2004; Adams *et al*., 2006). The microstructures of both CCTO ceramics were electrically heterogeneous, consisting of semiconductive grains with insulating layer of grain boundaries. Under an applied ac electric field, charges in the semiconducting grains were accumulated at the grain boundaries, producing the interfacial polarization at the interface between grain and grain boundary. This was responsible for the observed high dielectric response in both CCTO ceramics. From this electrical structure model, the effective dielectric constant could be expressed as $\varepsilon'_{eff} = \varepsilon_{gb} t_g / t_{gb}$, where ε_{gb}, t_g and t_{gb} were the dielectric constant of the grain boundary, the average grain size and the thickness of the grain boundary, respectively. A small increased in ε' of the CCTO-2 ceramic was obviously associated with the slight increase of the grain size, resulting from the increase of sintering temperature. Furthermore, it could be seen in (Figure 1) that the intensity of the diffraction peaks of both $CaTiO_3$ and CuO second phases of the CCTO-1 were higher than those observed in the CCTO-2. The existence of $CaTiO_3$ phase in both CCTO ceramics was clearly proved to be the cause of a decrease in ε' of CCTO ceramics (Ramirez *et al*., 2009). Therefore, the relatively low value of ε' in the CCTO-1 was also attributed to the high content of $CaTiO_3$ phase. It was interesting that the value of $\tan\delta$ is reduced by increasing sintering temperature, due to the higher grain boundary resistance (R_{gb}) of the CCTO-2 than that of the CCTO-1, as listed in (Table 2, Figure 3b) showed the frequency dependence of ε' on the temperature in the range of -50 to 200°C for CCTO-2. In this figure, it was observed that the variation of ε' value ($\Delta\varepsilon'$) at 1 kHz compared to the value at 30 °C for both CCTO-1 and CCTO-2 was found to be less than ±15% in the temperature range of -50 to 90 °C, as shown in the inset of (Figure 3b). However, the temperature variation of ε' was greater than ±15%, when the temperature was increased to a value higher than 90 °C.

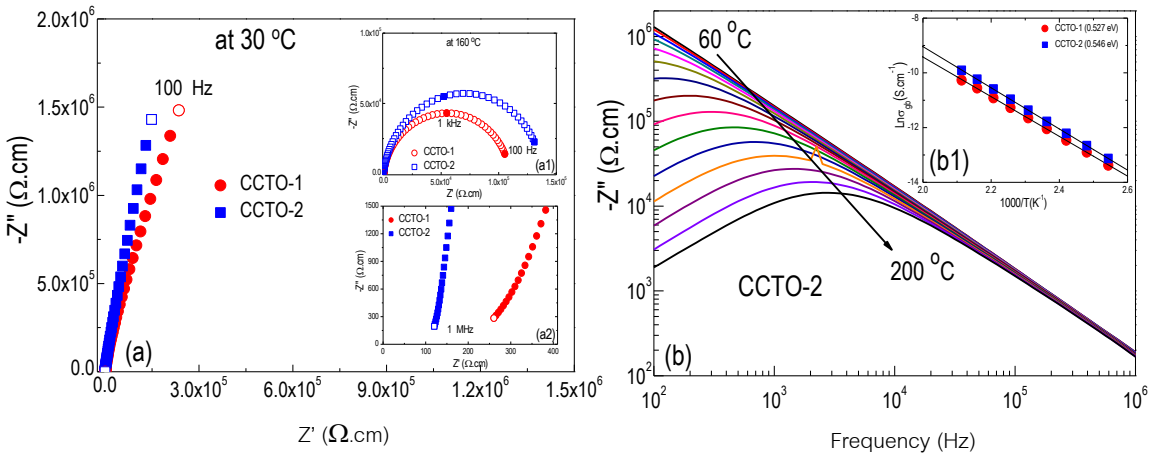

Figure 4 Impedance complex plane plot (Z^*) of CCTO-1 and CCTO-2 ceramics at (a) 30 °C, inset (a1) 160 °C. Inset (a2) is an expanded view of the high frequency at 30 °C for both CCTO ceramics. (b) The frequency dependence of Z'' in a temperature range of 60 - 200 °C for CCTO-2 ceramic. Inset (b1) shows the arrhenius plots of $\ln(\sigma_{gb})$ versus 1000/T for both of the CCTO ceramics.

Impedance complex plane plots (Z^*plots) of both ceramics at 30 °C, 160 °C and the expanded view of the highfrequency at 30 °C for CCTO-1 and CCTO-2 were shown in (Figure 4a), insets (a1) and (a2) of (Figure 4a), respectively. Generally, the grain resistance (R_g) and grain boundary (GB) resistance (R_{gb}) at a particular temperature for a polycrystalline ceramic could be determined from the diameter of two semicircular arcs observed in the impedance spectra in high and low frequency ranges, respectively (Sinclair *et al.*, 2002). In some cases, only the semicircular wearc at a low frequency range could be observed. In this work, R_g could be estimated from a nonzero intercept on the Z' axis at a high frequency (Sinclair *et al.*, 2002). Although the complete semicircular arcs of both CCTO ceramics at 30 °C could not be observed at the measurement frequency, the effect of sintering conditions on the electrical response of GBs was clearly seen at 160 °C inset (a1) of (Figure 4a). Although a nonzero intercept on the Z' axis can be observed in the inset (a2) of (Figure 4a), it was important to note that R_g could be estimated to be about 5 orders of magnitude smaller than R_{gb}. As a result, it was reasonable to suggest that both CCTO ceramics were electrically heterogeneous, consisting of semiconducting grains and insulating GBs. Consequently, base

on these experimental results, the giant ε' values of both CCTO ceramics couldan be attributed to the effect of their special heterogeneous microstructure i.e. the different electrical characteristics between the grain and GB were suggested as a major contribution to the observed giant ε'.

To investigate the electrical characteristic of grain boundaries, the frequency dependence of the imaginary part, Z'', of the complex impedance Z^* was performed and it couldan be calculated by the following equation,

$$Z^* = Z' - jZ'' = \frac{1}{j\omega\varepsilon^* C_0} \qquad (2)$$

Where Z' and Z'' are the real and imaginary parts of Z^*, respectively. C_0 was defined by ε_0 A/d. As shown in (Figure 4b), Z'' peak shifts to higher frequencies with increasing temperature, indicating a thermally activated electrical response. At the maximum value of Z'', it couldan be shown that $R = 2Z''_{\max}$ (Li *et al.*, 2009). Therefore, a decrease in $Z''_{\max}$ indicateds a decrease in either grain resistance or grain boundary resistance. At a temperature of 160 °C, the calculated R_{gb} values for CCTO-1 and CCTO-2 were 86.1 and 114.2 kΩ.cm, respectively. Base on these high calculated resistance values, relaxation peaks observed in (Figure 4b) should be considered as the electrical response of grain boundaries. It is important to note that the R_{gb} value of CCTO-2 is estimated to be 2 times higher than that of CCTO-1. The higher R_{gb} corresponds to a lower tanδ value of CCTO-2. This effect might be due to the relative density of each bulk CCTO ceramic (Table 1). As shown in the inset (b1) of (Figure 4b), the grain boundary conductivity $\sigma_{gb} = 1/R_{gb}$ follows the Arrhenius law,

$$\sigma_{gb} = \sigma_0 \exp\left(\frac{-E_{gb}}{k_B T}\right) \qquad (3)$$

Where σ_0 was the pre-exponential term, E_{gb} was the activation energy for the conduction at grain boundaries, k_B was the Boltzmann constant, and T was the absolute temperature. The values of E_{gb} for the CCTO-1 and CCTO-2 were calculated from the slopes of the plots of σ_{gb} vs. 1000/T. The E_{gb} values of CCTO-1 and CCTO-2 were found to be 0.527 and 0.546 eV, respectively. These two values were comparable to those reported in the literatures of 0.662 eV (Adams *et al.*, 2006). As a result, it was obvious that the E_{gb} value of CCTO-2 was higher than that of the CCTO-1. This result corresponds to the observation for the higher dielectric constant of CCTO-2, as shown in (Figure 3a).

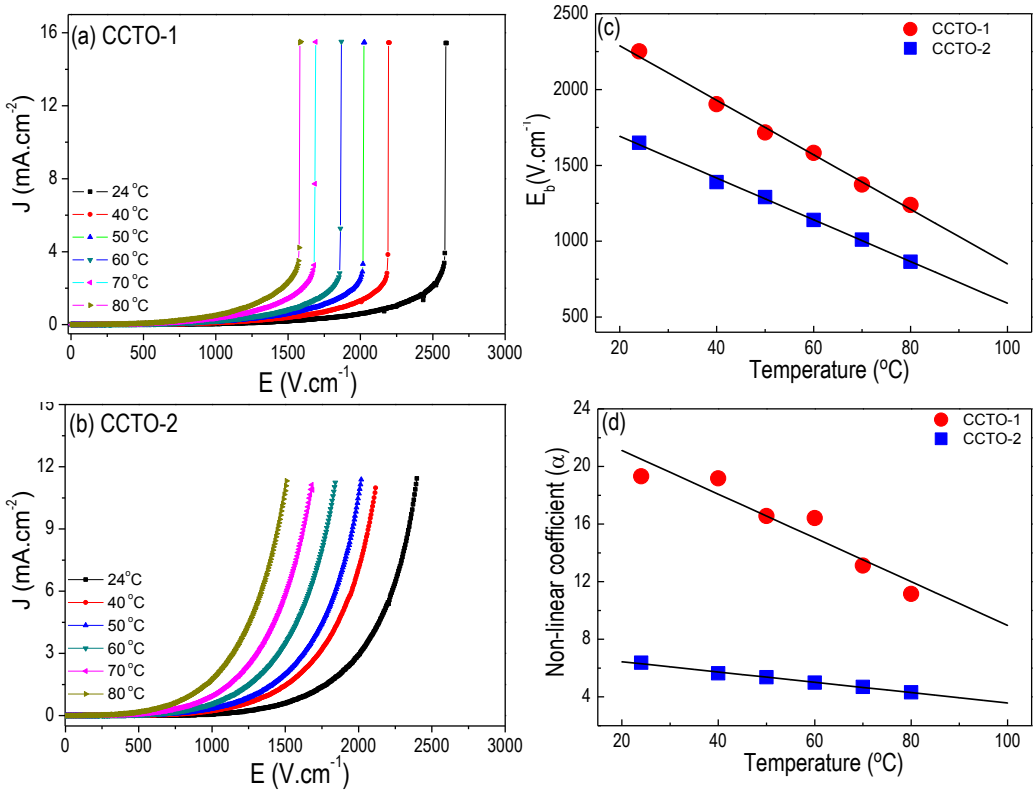

Figure 5 *J-E* characteristics of (a) CCTO-1 and (b) CCTO-2 ceramics at various temperatures. (c), (d) displays the temperature dependence of the breakdown field (E_b) and nonlinear coefficient (α) of CCTO-1 and CCTO-2 ceramics, respectively.

To further understanding on the electrical response of grain boundaries of both CCTO ceramics, non-Ohmic characteristics were investigated at various temperatures. The current density–electric field strength (*J–E*) characteristics of the CCTO-1 and CCTO-2 in a temperature range of 24 to 80 °C are shown in (Figure 5a and 5b), respectively. In (Figure 5a and 5b), both CCTO ceramics exhibit non-Ohmic properties, similar to those reported by other groups (Fang *et al.*, 2006; Felix *et al.*, 2011). The two most important parameters related to the non-Ohmic properties, i.e. the nonlinear coefficient (α) and the breakdown field (E_b), for both CCTO ceramics can be calculated from these *J–E* curves. It was important to note that at 24 °C, the α values were determined in the range of 1–10 mA.cm^2 and found to be 19.31 and 6.37 for the CCTO-1 and CCTO-2, respectively. The E_b values were obtained at J = 1 mA.cm^{-2} and found to be 2,215

and 1,010 V.cm^{-1} for the CCTO-1 and CCTO-2, respectively. As couldan be seen in (Figure 5c and 5d), the E_b and α values of both CCTO ceramics decrease with the increase of measuring and sintering temperature, indicating the effect of temperature on the Schottky barrier (Felix *et al*., 2011). It was worth noting that the value of E_b for the CCTO-2 was lower than that of the CCTO-1. This result correspondeds to the observation of a higher grain boundary conductivity for the CCTO-2, as shown in the inset (a2) of (Figure 4.) It was previously reported by Fang *et al*. (2006) that the increase of the grain boundary resistance (R_{gb}) depends on the concentration of the CuO second phase. Therefore, the slight decrease of CuO secondary phase in both CCTO ceramics, as revealed by the XRD results in (Figure 1), couldan be one of the most important factor that affect the *J-E* characteristics of both CCTO ceramics.

Conclusions

CCTO nanopowder of perovskite structure as revealed by the XRD results couldan be successfully prepared by calcination the CCTO precursor powder obtained by the aloe vera solution method at 850 °C for 4 h in air. The second phases of $CaTiO_3$ and CuO were found in the precursor powder. CCTO-1 and CCTO-2 ceramics were prepared by sintering the obtained CCTO nanopowder at a temperature of 1020 and 1050 °C for 6 h in air, respectively. The XRD results indicated the perovskite structure of both ceramics with the observed second phases of $CaTiO_3$ and CuO. Increasing sintering temperature couldan reduce the second phase and increase the grain size of the CCTO ceramic. From the dielectric measurements, it was found that higher sintering temperature couldan result in the higher ε' with low tanδ. CCTO-2 ceramic particularly exhibits the giant ε' value of about 11,000 with the low tanδ value of 0.077 at 30 °C and 1 kHz. The CCTO-1 ceramic exhibits high values of α (19.31) and E_b (2,215 V.cm^{-2}). These parameters were closely related to the sintering temperature, dielectric properties and grain boundary resistance (R_{gb}) that couldan be attributed to the variation in the height of the Schottky barriers.

Acknowledgments

This work was financially supported by Rajamangala University of Technology Rattanakosin, Wang Klai Kangwon Campus, Thailand (Grant No. A13/2560).

References

Adams, T.B., D.C. Sinclair and A.R. West. 2006. Influence of processing conditions on the electrical properties of $CaCu_3Ti_4O_{12}$ ceramics. *J. Am. Ceram. Soc. 89*: 3129-3125.

Amalraj, A.J., J.W. Sahayaraj, C. Kumar, S. Rajendran, A.P.P. Regis, S.K. Selvaraj and R. Mohan. 2013. Corrosion inhibitor aloe vera-nikel system controlling the corrosion of carbon steel in rain water. *Eur. Chem. Bull. 2*: 315-319.

Capsoni, D., M. Bini, V. Massarotti, G. Chiodelli, M.C. Mozzatic and C.B. Azzoni. 2004. Role of doping and CuO segregation in improving the giant permittivity of $CaCu_3Ti_4O_{12}$. *J. Solid State Chem. 177*: 4494-4500.

Chandran, S.P., M. Chaudhary, R. Pasricha, A. Ahmad and M. Sastry. 2006. Synthesis of gold nanotriangles and silver nanoparticles using Aloe vera plant extract. *Biotechnol. Progr. 22*: 577-583.

Choi, S. and M.H. Chung. 2003. A review on the relationship between aloe vera components and their biologic effects. *Seminar Integrat Med. 1*: 53-62.

Chung, S.-Y., I.-D. Kim and S.-J.L. Kang. 2004. Strong non-linear current–voltage behaviour in perovskite-derivative calcium copper titanate. *Nat. Mater. 3*: 774-778.

De Almeida, S., C. Autret, A. Lucas, C. Honstettre, F. Pacreau and F. Gervais. 2014. Leading role of grain boundaries in colossal permittivity of doped and undoped CCTO. *J. Eur. Ceram. Soc. 34*: 3649-3654.

Fang, T.T., L.T. Mei and H.F. Ho. 2006. Effects of Cu stoichiometry on the microstructures, barrier-layer structures, electrical conduction, dielectric responses and stability of $CaCu_3Ti_4O_{12}$. *Acta Mater. 54*: 2867-2875.

Felix, A.A. M.O. Orlandi and J.A. Varela. 2011. Schottky-type grain boundaries in CCTO ceramics. *Solid State Commun.151*: 1377-1381.

Guillemet-Fritsch, S., T. Lebey, M. Boulos and B. Durand. 2006. Dielectric properties of $CaCu_3Ti_4O_{12}$ based multiphased ceramics. *J. Eur. Ceram. Soc. 26*: 1245-1257.

Homes, C.C., T. Vogt, S.M. Shapiro, S. Wakimoto and A.P. Ramirez. 2001. Optical response of high-dielectric constant perovskite related oxide. *Science*, *293*: 673-676.

Jesurani, S., S. Kanagesan, R. Velmurugan, C. Thirupathi, M. Sivakumar and T. Kalaivani. 2011. Nanoparticles of the giant dielectric material, calcium copper titanate from a sol–gel technique. *Mater. Lett. 65*: 3305-3308.

Jha, P., A.K. Arora and P. Ganguli. 2003. Polymeric citrate precursor route to the synthesis of the high dielectric constant oxide, $CaCu_3Ti_4O_{12}$. *Mater. Lett. 57*: 2443-2446.

Jin, S., H. Xia, Y. Zhang, J. Guo and J. Xu. 2007. Synthesis of $CaCu_3Ti_4O_{12}$ ceramic via a sol-gel method. *Mater. Lett. 6*: 1404-1407.

Klinkaewnarong, J., E. Swatsitang, C. Masingboon, S. Seraphin and S. Maensiri. 2010. Synthesis and characterization of nanocrystalline HAp powders prepared by using aloe vera plant extracted solution. *Curr. Appl Phys. 10*: 521-525.

Krohns, S., P. Lunkenheimer, S.G. Ebbinghaus and A. Loidl. 2008. Colossal dielectric constants in single-crystalline and ceramics $CaCu_3Ti_4O_{12}$ investigated by broadband dielectric spectroscopy. *J. Appl. Phys. 103*: 084107.

Laokul, P., S. Serapin, V. Amornkitbamrung and S. Maensiri. 2011. Characterization and magnetic properties of nanocrystalline $CuFe_2O_4$, $NiFe_2O_4$, $ZnFe_2O_4$ powders prepared by the Aloe vera extract solution. *Curr. Appl Phys. 11*: 101-108.

Li, M., A. Feteira and D.C. Sinclair. 2009. Relaxor ferroelectric-like high effective permittivity in leaky dielectrics/oxide semiconductors induced by electrode effects: A case study of CuO ceramics. *J. Appl. Phys. 105*: 114109.

Liu, J., Y. Sui, C. Duan, W.N. Mei, R.W. Smith and J.R. Hardy. 2006. $CaCu_3Ti_4O_{12}$: Low-temperature synthesis by pyrolysis of an organic solution. *Chem. Mater. 18*: 3878-3882.

Liu, L., L. Fang, Y. Huang, Y. Li, D. Shi, S. Zheng, S. Wu and C. Hu. 2011. Dielectric and nonlinear current–voltage characteristics of rare–earth doped $CaCu_3Ti_4O_{12}$ ceramics. *J. Appl. Phys. 110*: 094101.

Lunkenheimer, P., S. Krohns, R. Fichtl, S.G. Ebbinghaus, A. Reller and A. Loidl. 2010. Colossal dielectric constants in transition-metal oxides.*Eur. Phys. J. Special Topics.180*: 61-89.

Maensiri, S., P. Laokul, J. Klinkaewnarong, S. Phokha, V. Promarak and S. Seraphin. 2008. Indium oxide (In_2O_3) nanoparticles using Aloe vera plant extract: Synthesis and optical properties. *Optoelectron. Adv. Mater. Rapid Commun. 10*: 161-165.

Mu, C.H., P. Liu, Y. He, J.P. Zhou and H.W. Zhang. 2009. An effective method to decrease dielectric loss of $CaCu_3Ti_4O_{12}$ ceramics. *J. Alloys Compd. 471*: 137-141.

Ni, L. and X.M. Chen. 2007. Structure and modified giant dielectric response in $CaCu_3(Ti_{1-x}Sn_x)_4O_{12}$ ceramics. *Mater Chem Phys. 124*: 982-986.

Ramirez, M.A., P.R. Bueno, R. Tararam, A.A. Cavalheiro, E. Longo and J.A. Varela. 2009. Evaluation of the effect of the stoichiometric ratio of Ca/Cu on the electrical and microstructural properties of the $CaCu_3Ti_4O_{12}$ polycrystalline system. *J. Phys. D: Appl. Phys. 42*: 185503.

Reynolds, T. and A.C. Dweck. 1999. Aloe vera leaf gel: a review update. *J. Ethnopharmacol. 68*: 3-37.

Sinclair, D.C., T.B. Adams, F.D. Morrison and A.R. West. 2002. One-step internal barrier layer capacitor. *Appl. Phys. Lett. 80*: 2153.

Subramanian, M.A., D. Li, N. Duan, B.A. Reisner and A.W. Sleight. 2000. High dielectric constant in $ACu_3Ti_4O_{12}$ and $ACu_3Ti_3FeO_{12}$ phases. *J. Solid State Chem. 151*: 323-325.

Thongbai, P., B. Putasaeng, T. Yamwong and S. Maensiri. 2012. Current-voltage nonlinear and dielectric properties of $CaCu_3Ti_4O_{12}$ ceramics prepared by a simple thermal decomposition method. *J. Mater. Sci: Mater. Electron. 23*: 795-801.

Xue, R., Z. Chen, H. Dai, D. Liu, T. Li and G. Zhao. 2015. Effects of rare earth ionic doping on microstructures and electrical properties of $CaCu_3Ti_4O_{12}$ ceramics. *Mater. Res. Bull. 66*: 254-26